Supplementary Information

Layer-Stacked NiO Nanowire/Nanosheet Homostructure for Electrochromic Smart Windows with Ultra-Large Optical Modulation

Yi Gao,[a] Pengyang Lei,[a] Siyu Zhang,[a] Huanhuan Liu,[a] Chengyu Hu,[a] Zhu Kou,[a] Jinhui Wang*[a] and Guofa Cai*[a]

[a,] Key Laboratory for Special Functional Materials of Ministry of Education, National & Local Joint Engineering Research Center for High-efficiency Display and Lighting Technology, School of Materials and Engineering, and Collaborative Innovation Center of Nano Functional Materials and Applications, Henan University, Kaifeng 475004, China

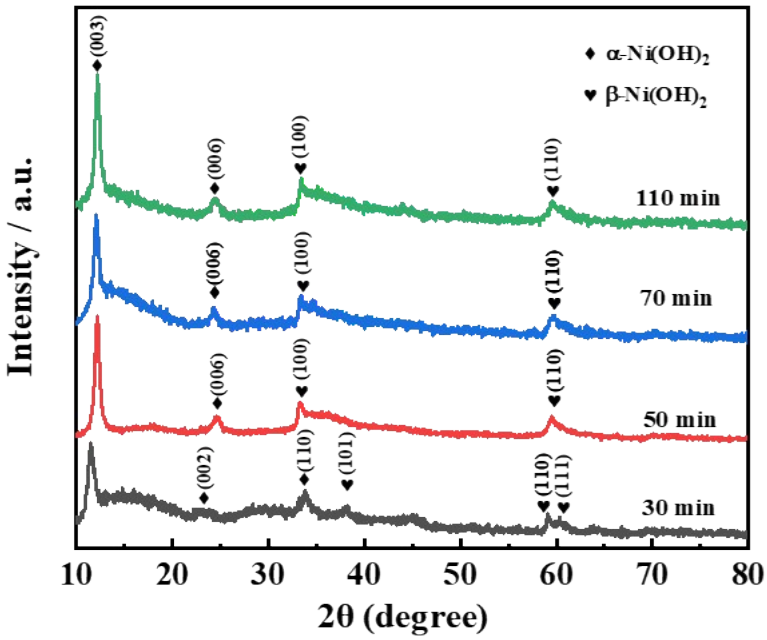

Fig. S1 XRD patterns of grown $Ni(OH)_2$.

The synthesized product is mainly a mixture of α-$Ni(OH)_2$ and β-$Ni(OH)_2$, which is confirmed by X-ray diffraction (XRD) patterns (Fig. S1). With the increase in reaction time, $Ni(OH)_2$ grows along the (003) plane of the α phase.

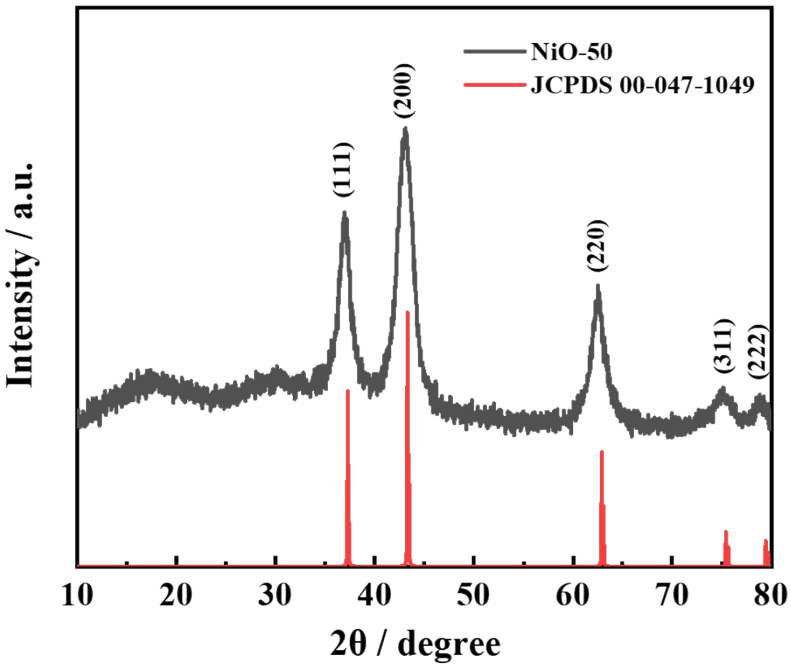

Fig. S2 XRD patterns of as-prepared NiO-50 film.

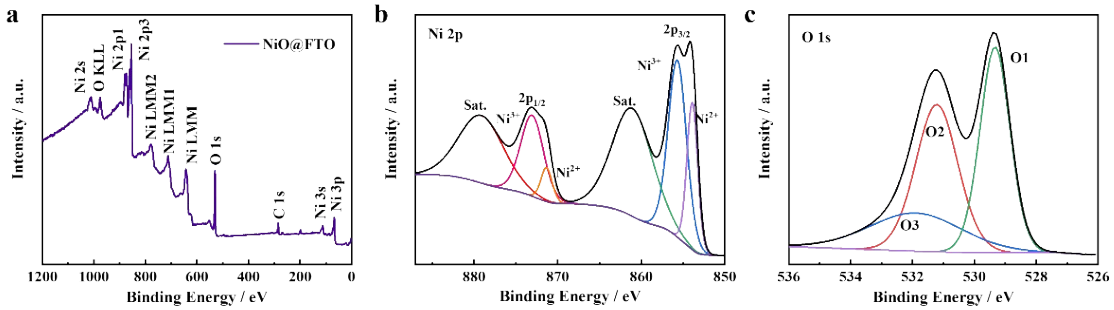

Fig. S3 XPS spectra of NiO-50 film. (a) Full survey spectrum. (b) Ni 2p region. (c) O 1s region.

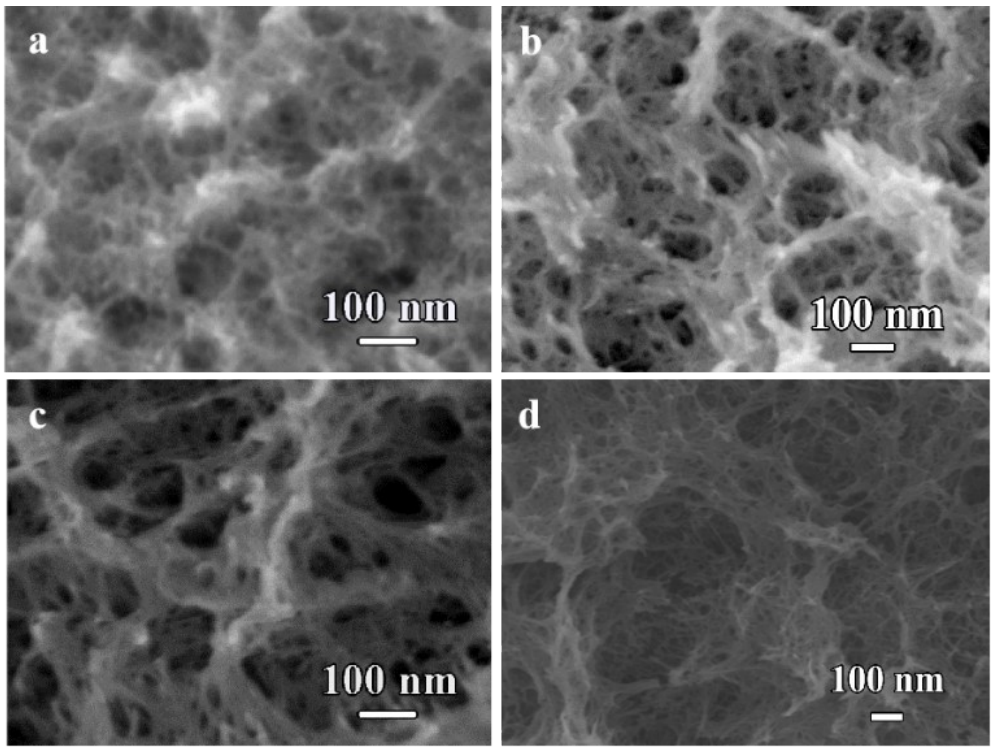

Fig. S4 SEM images of NiO films were hydrothermally grown at (a) 35, (b) 70, (c) 90, and (d) 110 min.

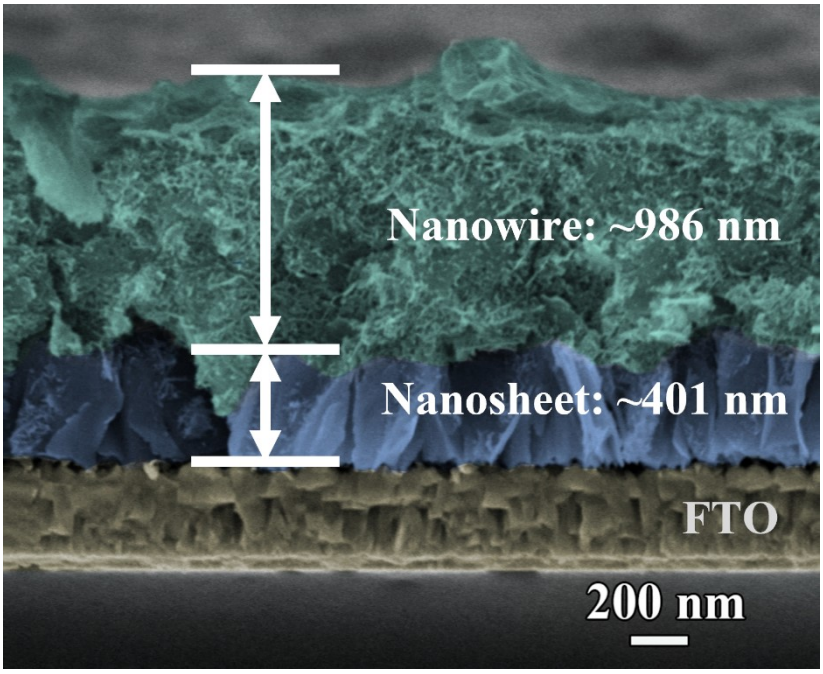

Fig. S5 Cross-section of NiO-110 thin film.

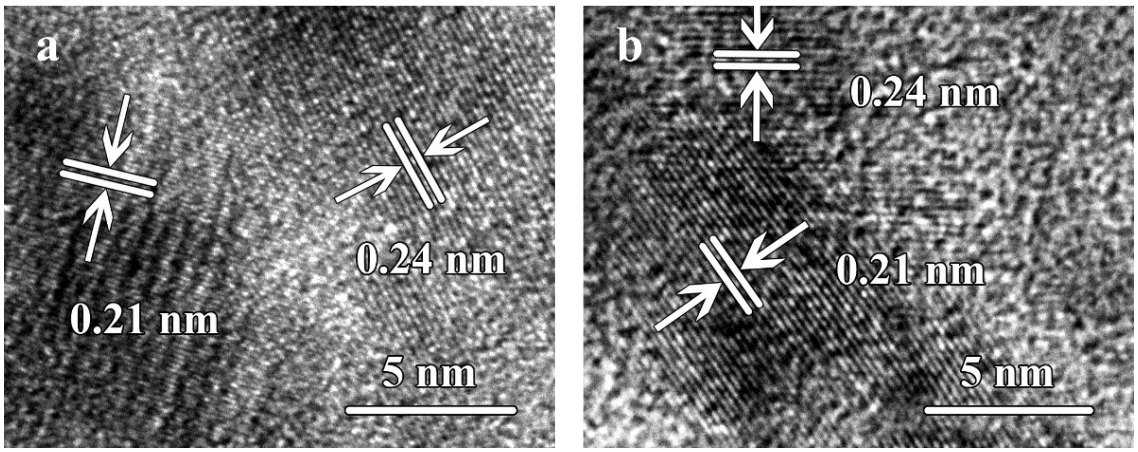

Fig. S6 HRTEM images of NiO-30 and NiO-50 films, respectively.

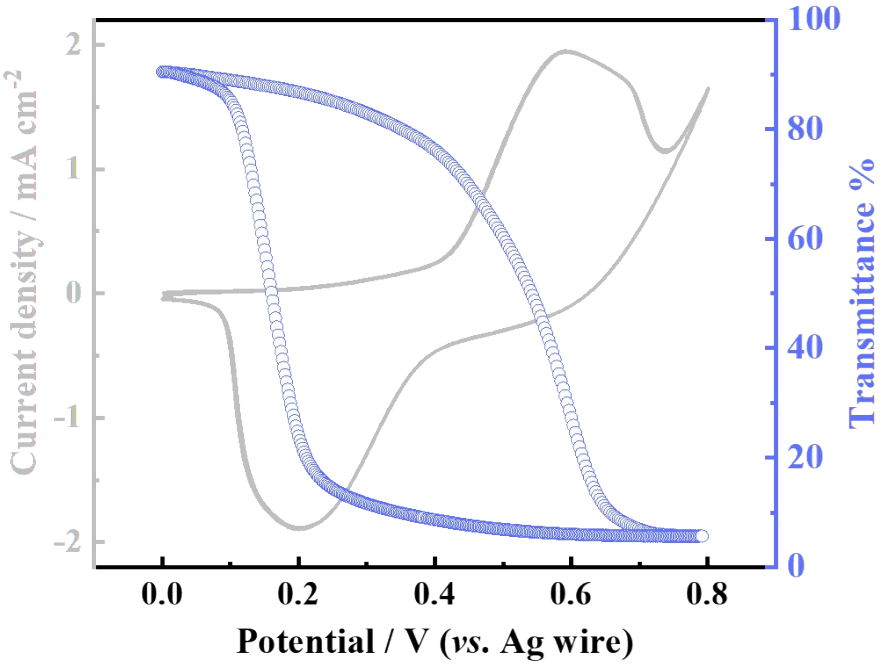

Fig. S7 CV curve and in-situ dynamic transmission spectrum of d NiO-50 at 550 nm at a scan rate of 10 mV s^{-1}.

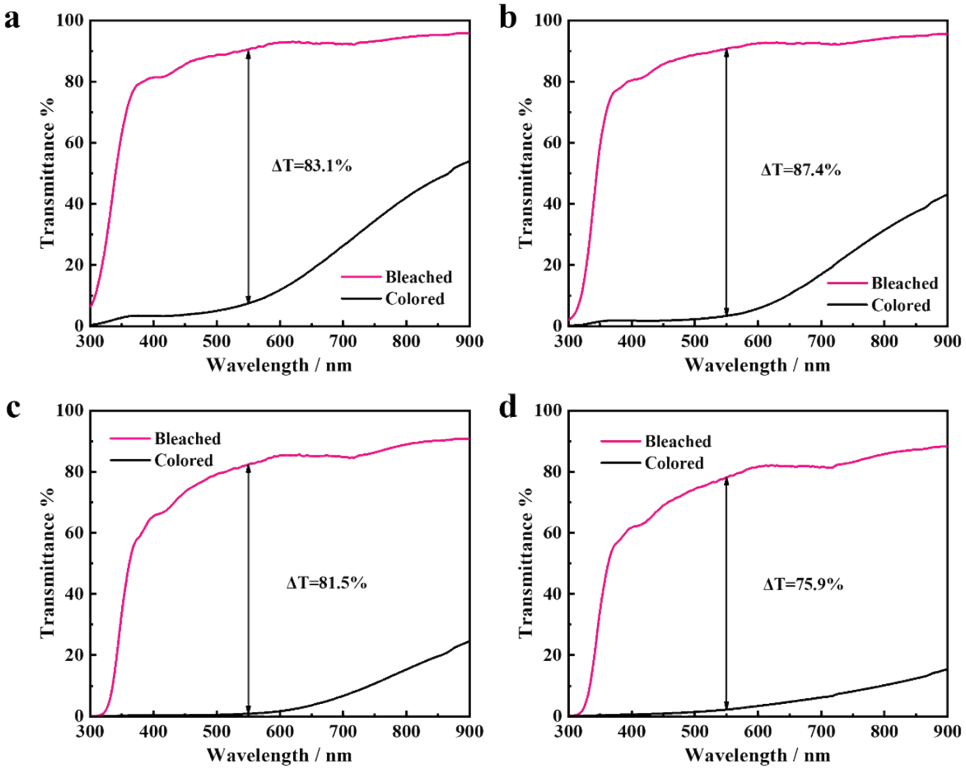

Fig. S8 Optical transmission spectra of (a) NiO-35, (b) NiO-70, (c) NiO-90, (d) NiO-110 films, respectively.

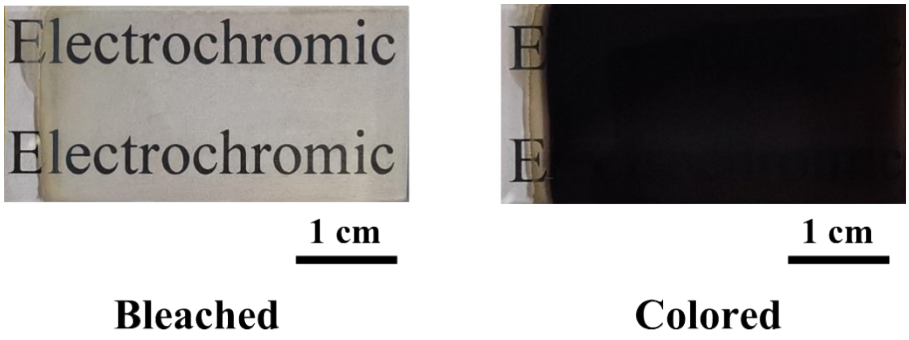

Fig. S9 Digital photos of the NiO film in bleached and colored states.

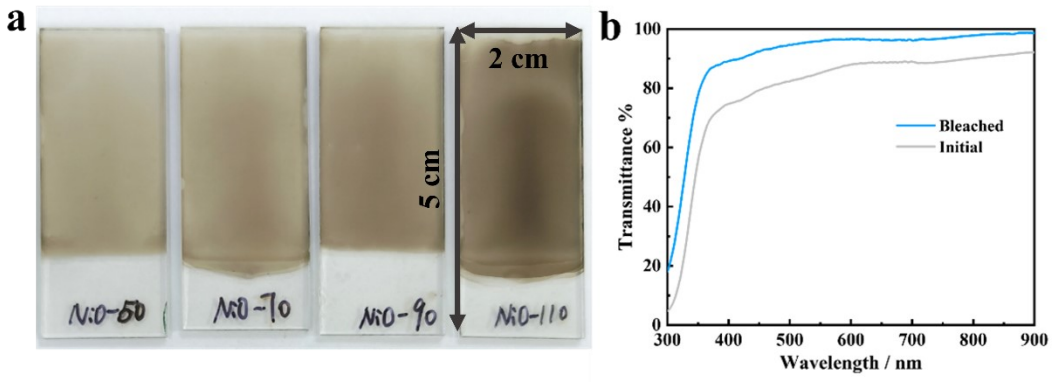

Fig. S10 (a) Digital photos of the NiO-50 to NiO-110 films in their initial states; (b) The transmittance comparison of NiO-50 film in the bleached and initial states.

As shown in Fig. S10a, NiO films in their initial state show an intrinsic yellow color, wherein the color deepens with the NiO growth from NiO-50 to NiO-110. It is noted that the NiO transmittance in the bleached state is generally higher than that in the initial state by comparison of NiO-50 film in Fig. S10b, due to the existence of multiple valences in the initial state (Fig. S3b).

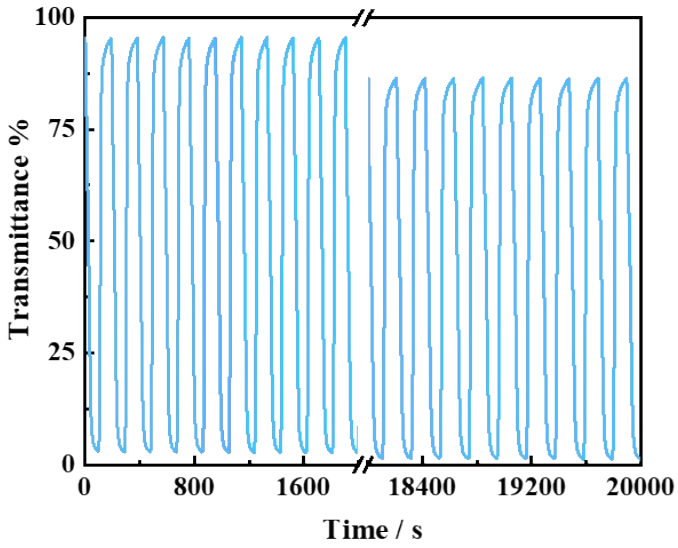

Fig. S11 In situ transmission spectrum at 0 V and 0.7 V (*vs.* Ag wire) square wave potential for 100 s corresponding to the first and last ten cycles of NiO-50 in 1000 cycles.

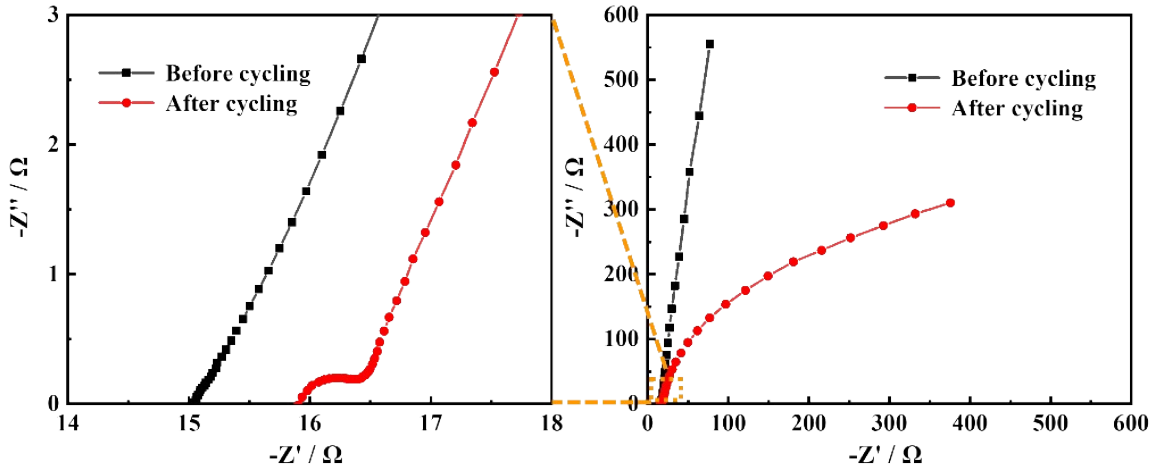

Fig. S12 Nyquist plots of the NiO-50 film before and after cycling measurement by applying the frequency from 0.01 Hz to 100000 Hz.

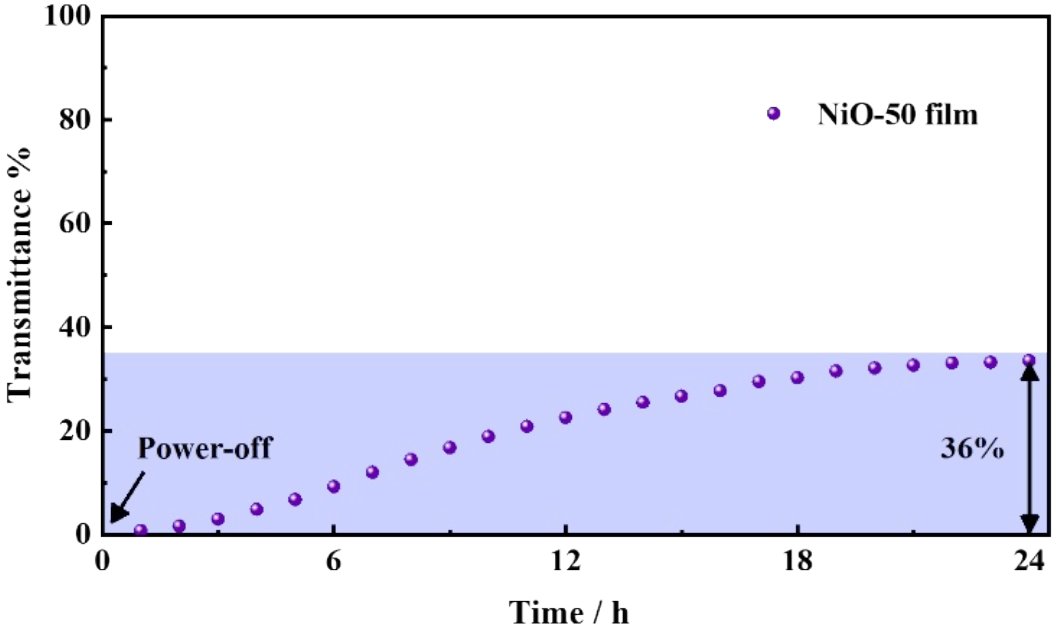

Fig. S13 The transmittance spectrum of NiO-50 film at 550 nm after a coloring voltage of 0.7 V (*vs*. Ag wire) was applied.

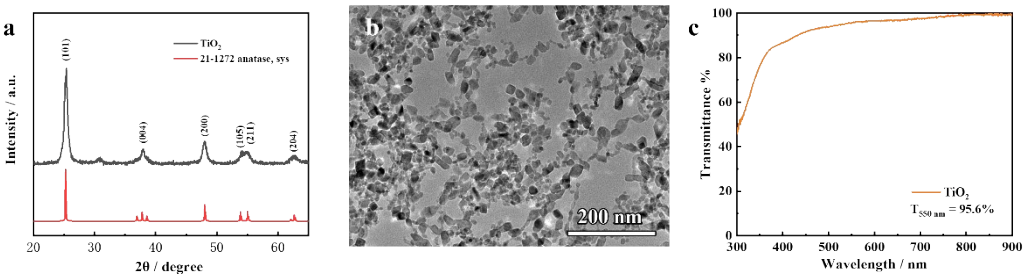

Fig. S14 Characterization of TiO_2 nanoparticles film fabricated by electrostatic spraying method: (a) The XRD pattern of TiO_2 film on FTO substrate. (b) TEM image of TiO_2 nanoparticles. (c) The transmittance spectrum of TiO_2 film.

These results confirmed that the successful preparation of anatase-phase TiO_2 in the form of 10-45 nm nanoparticles.

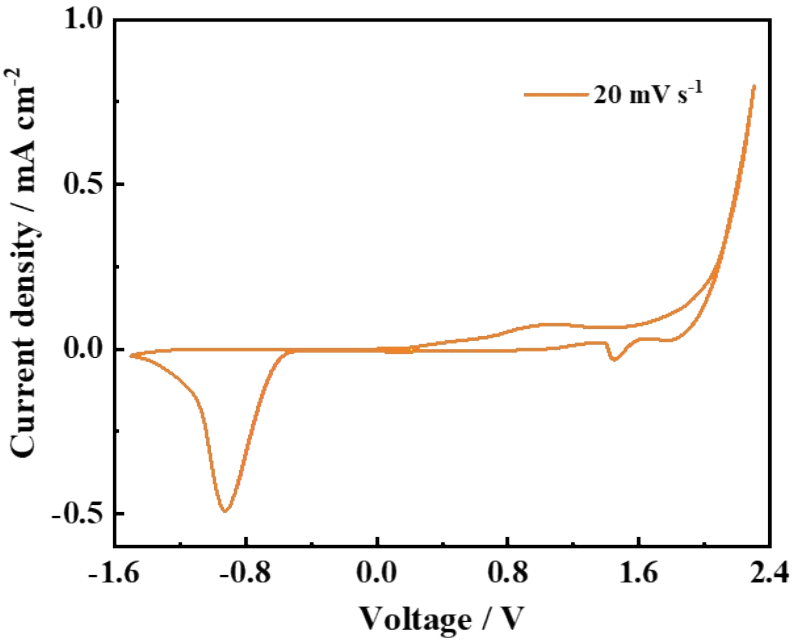

Fig. S15 CV curve of the assembled electrochromic device at 20 mV s^{-1}.

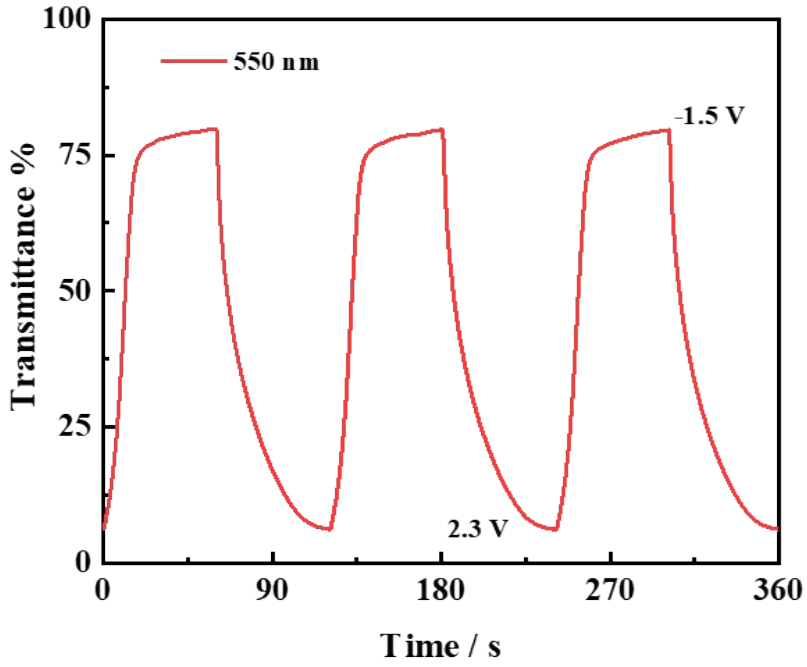

Fig. S16 The in-situ transmittance response at 550 nm which was obtained by applying square wave voltages of -1.5 V and 2.3 V for 60 s.

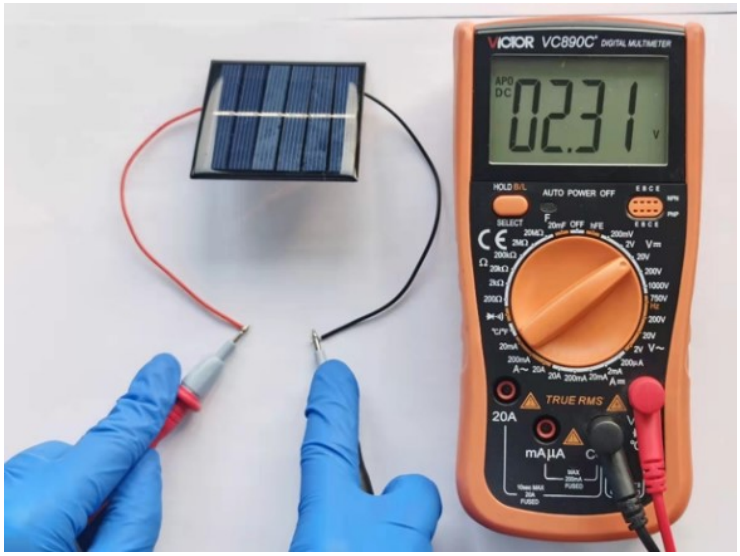

Fig. S17 Demonstration of commercial silicon solar panels with an output voltage of 2.31 V.

Table S1 Comparison of the response time of NiO film under different hydrothermal reaction times.

Sample	t_b / **s**	t_c / **s**
NiO-30	3.4	4.3
NiO-35	8.7	12
NiO-50	9.5	12.2
NiO-70	17.7	13.7
NiO-90	14.1	12.9
NiO-110	14	12.6

Table S2 Comparison of electrochromic performance of NiO-50 and other NiO EC films.

Method	ΔT / %	t_b, t_c / s	Cycling stability	CE / cm^2 C^{-1}	References
Sol-gel	51 (550 nm)	7/5	3000 (90% of retention)	40	*J. Mater. Chem. C*, **2018**, *6*, 4952
Sol-gel	54.27 (450 nm)	3.2/2.7	-	48.5	*Appl. Surf. Sci.*, **2021**, *537*, 147902
Template	78.5 (550 nm)	3.92/3.43	1000 (78% of retention)	51.8	*Surf. Coat. Technol.*, **2018**, *337*, 63
Hot-filament metal-oxide vapor deposition (HFMOVD)	60 (630 nm)	1.55/1.22	1000 (78.3% of retention)	43.3	*Sol. Energy Mater. Sol. Cells*, **2013**, *112*, 91
Electrodeposition	76 (550 nm)	3/6	3000 (61% of retention)	46	*Electrochim. Acta*, **2011**, *56*, 1208
E-beam evaporation	66 (630 nm)	6.3/4.4	-	55	*Sol. Energy Mater. Sol. Cells*, **2014**, *120*, 109
E-beam evaporation	27.2 (540 nm)	-	800 (78% of retention)	53.1	*J. Sci.: Adv. Mater. Devices*, **2017**, *2*, 225
Hydrothermal	67 (550 nm)	5.2/6.6	600 (40% of retention)	92	*J. Mater. Chem. A*, **2013**, *1*, 4286
Chemical bath deposition	36 (630 nm)	9.03/38.87	2000 (91.95% of retention)	16.95	*ACS Appl. Mater. Interfaces*, **2021**, *13*, 57403
Radio frequency magnetron sputtering	67.6 (550 nm)	3.1/2.1	1000 (Activating all the time)	51.6	*Appl. Surf. Sci.*, **2018**, *451*, 104
Solvothermal	63.6 (550 nm)	11.5/9.5	1000 (90.8% of retention) / 5000 (56.4% of retention)	42.8	*Nano Energy*, **2015**, *12*, 258
Hydrothermal	95 (550 nm)	5.4/9.8	700 (61% of retention)	91.2	*Nanoscale Adv.*, **2022**, *4*, 4748
Hydrothermal	77 (550 nm)	2/2.5	3000 (70% of retention)	49	*Electrochim. Acta*, **2013**, *111*, 86

Hydrothermal	40 (632.8 nm)	1.8/2.7	-	63.2	*J. Mater. Chem. A*, **2015**, *3*,20614
Hydrothermal	93.4 (550 nm)	9.5/12.2	1000 (91.2% of retention)	72.1	**This work**

Table S3 Comparison of electrochromic performance of NiO-based EC devices.

Device	**ΔT / %**	**t_b , t_c / s**	**Cycling**	**CE / cm^2 C^{-1}**	**References**
NiO||TiO_2	74	-	-	61.5	*J. Phys. Chem. Lett.*, **2023**, *14*, 2284
WO_3||NiO	75	10/13.1	100	131.9	*Nanoscale*, **2016**, *8*, 348
AgNWs||NiO	14.3	-	2000	51.9	*Adv. Energy Mater.*, **2018**, *8*, 1800069
NiO||FTO	47	6.7/2.7	-	85.3	*J. Solid State Electrochem.*, **2021**, *25*, 821
WO_3||NiO	46	3.1/4.6	2500	90	*Sci. Rep.*, **2020**, *10*, 8430
NiO||$Li_4Ti_5O_{12}$	55	7.4/6.5	600	-	*J. Mater. Chem. A*, **2021**, *9*, 6451
NiO||MnO_2	57	12/12.1	200	28.5	*J. Mater. Chem. C*, **2021**, *9*, 14378
NiO||TiO_2	80.3	34.8/34.2	-	31.7	**This work**